









ORIGINAL RESEARCH

NDUFAF3 is Involved in the Assembly of the Q/P Modules of Respiratory Complex I in the Green Microalga *Chlamydomonas reinhardtii*

Thalia Salinas-Giegé¹  | Mitchell Ticoras^{2,3}  | Florent Waltz⁴  | Nadine Coosemans² | Steven Fanara⁵  | Johana Chicher⁶  | Philippe Hammann⁶  | Patrice P. Hamel³  | Claire Remacle² 

¹Institut de biologie moléculaire des plantes, CNRS, Université de Strasbourg, Strasbourg, France | ²Genetics and Physiology of Microalgae, InBioS/Phytosystems Research Unit, University of Liège, Liège, Belgium | ³Department of Molecular Genetics, The Ohio State University, Columbus, Ohio, USA | ⁴Biozentrum, University of Basel, Basel, Switzerland | ⁵Functional Genomics and Plant Molecular Imaging, InBioS/Phytosystems Research Unit, University of Liège, Liège, Belgium | ⁶Plateforme Protéomique Strasbourg-Esplanade, Institut de Biologie Moléculaire et Cellulaire, UAR1589 du CNRS, Strasbourg Cedex, France

Correspondence: Claire Remacle (c.remacle@uliege.be)

Received: 17 April 2025 | **Revised:** 25 June 2025 | **Accepted:** 30 June 2025

Handling Editor: H. Mireau

Funding: This work was supported by FNRS-FWO EOS Project (30829584 [to C.R.]), FNRS CDR (J.0175.20 and J.0149.23 [to C.R.]), Action de Recherche Concertée from the University of Liège (DARKMET ARC grant 17/2108 [to C.R.]). F.W. acknowledges the Alexander von Humboldt (AvH) foundation for the Humboldt Research Fellowship for Postdocs and the Swiss National Science Foundation (SNSF) for the Swiss Postdoctoral Fellowship (project 210561). M.T. acknowledges funding from the Department of Molecular Genetics at The Ohio State University (Berl Oakley award), Erasmus+ mobility funds (to C.R. and P.H.), and financial support from STILSA (Students in Life Sciences Abroad). T.S.-G. acknowledges the Agence Nationale de la Recherche (ANR) grant (ARAMIS, ANR-21-CE12-0012, ANR-10-IDEX-0002, ANR-20-SFRI-0012, ANR-17-EURE-0023 and ANR-11-EQPX-0022). The mass spectrometer purchase was supported by the Interdisciplinary Thematic Institute IMCBio+, as part of the ITI 2021–2028 program of the University of Strasbourg, CNRS, and Inserm, under the framework of the French Investments of the France 2030 Program. Further funding support was from the Région Grand Est CPER2021–2027 (ImaProGen Project) and the Strasbourg Eurometropole.

Keywords: assembly factor | *Chlamydomonas* | complex I | mitochondrial respiratory chain | NDUFAF3

ABSTRACT

The mitochondrial NADH:ubiquinone oxidoreductase, or complex I, is composed of a hydrophobic arm comprising the P module and a hydrophilic arm comprising the N and Q modules. The assembly of complex I is well characterized in humans and is catalyzed by a series of assembly factors that join the Q, P, and N modules sequentially. The complex I of protists and plants, however, contains additional ancestral features, namely a ferredoxin bridge that connects the matrix and the membrane arms and a γ carbonic anhydrase domain, whose mechanisms of assembly are unknown. In this work, a strain where the complex I assembly factor NDUFAF3 has been tagged with a 3 \times FLAG at the C-terminus is investigated in the green microalga *Chlamydomonas reinhardtii*. Like its human homolog, NDUFAF3 interacts strongly with the classical subunits of the Q and P modules, but also with the γ carbonic anhydrase domain and C1-FDX, a subunit of the ferredoxin bridge. The predicted structural positioning of NDUFAF3 within the Q module suggests a role in the formation of this bridge. In contrast, subunits of the N module are only loosely associated with NDUFAF3. We further demonstrate that the N module is attached at a later stage of assembly, suggesting that *Chlamydomonas* complex I assembles in a human-like sequence. This contrasts with what is documented in Angiosperms, where the N and Q modules are attached together before anchoring to the P module. Altogether, these results highlight a conserved and ancestral role of NDUFAF3 in complex I manufacture.

1 | Introduction

Mitochondrial oxidative phosphorylation drives the synthesis of ATP within eukaryotic cells. This process involves five multisubunit complexes: four oxidoreductases (complexes I–IV) and ATP synthase (complex V). NADH:ubiquinone oxidoreductase (complex I) is the main entry point of electrons into the respiratory chain. It catalyzes NADH oxidation and connects ubiquinone reduction to proton pumping from the matrix side to the intermembrane space of the mitochondrion. In eukaryotes, such as the green microalga *Chlamydomonas reinhardtii* (henceforth *Chlamydomonas*) (Cardol et al. 2004; Waltz et al. 2025), complex I is approximately 1 MDa and consists of about 50 subunits, of which 14 core subunits are of bacterial origin. X-ray and cryo-EM analyses revealed that complex I is composed of two arms, structured into an L-shape in all organisms examined so far (reviewed in Galemou Yoga et al. 2020) (Figure 1A). The hydrophilic arm protrudes into the mitochondrial matrix, and it is composed of the N module (NADH dehydrogenase) and the Q module (ubiquinone reduction), both of which together harbor critical prosthetic groups (8 Fe–S clusters, 1 flavin mononucleotide). The membrane arm is involved in proton translocation (P) and is divided into two modules, one proximal (P_p) and one distal (P_d) with respect to the location of the peripheral arm (Figure 1A). The hydrophobic arm contributes to proton pumping by a mechanism hypothesized to rely on a long-range propagation of conformational rearrangements driven by ubiquinone reduction (Kampjut and Sazanov 2020). In many protists (Zhou et al. 2022; Mühleip et al. 2023) and photosynthetic eukaryotes, including *Chlamydomonas*, an additional matrix-exposed domain attached to the P_p module of the membrane arm is composed of γ carbonic anhydrase subunits (Dudkina et al. 2008; Perales et al. 2004; Sunderhaus et al. 2006; Fromm et al. 2016; Soufari et al. 2020; Klusch et al. 2021; Waltz et al. 2025). In addition, a bridge connects the two arms of plant complex I between the Q module and the γ carbonic anhydrase domain (Figure 1A). The bridge contains a ferredoxin-like protein (C1-FDX), which plays a critical role in the establishment of the connection (Klusch et al. 2021). Together with the γ carbonic anhydrase domain, this bridge is considered a conserved and ancestral feature of complex I in protists, green algae, and land plants, lost in fungi and mammal complex I (Braun and Klusch 2024).

Complex I formation begins with the independent assembly of the four modules (N, Q, P_d , and P_p) described above. These modules are then further combined in a stepwise manner to yield the active holoenzyme. The modular assembly has been extensively investigated in humans (Guerrero-Castillo et al. 2017; Stroud et al. 2016) and, to a lesser extent, in plants where *Arabidopsis thaliana* has remained the model of investigation (Ligas et al. 2019). Complex I assembly is grosso modo conserved in the two model organisms, but some differences do exist, for example, at the matrix arm level. The matrix arm is fully assembled before connecting to the P_p module in *Arabidopsis*. In humans, the Q module is first connected to the P_p module. Then, the membrane arm is formed by integrating the P_d module before the N module is connected last to the structure. Two assembly intermediates, corresponding to 200 and 700 kDa, have been identified in the green microalga *Chlamydomonas*. The 200 kDa

module is soluble and exhibits NADH dehydrogenase activity (Cardol et al. 2002). The 700 kDa subcomplex contains the matrix arm, the P_p module, and the γ carbonic anhydrase module and is accumulated when subunits of the P_d module are absent (Barbieri et al. 2011; Cardol et al. 2008, 2002, 2006).

Numerous assembly factors participate in complex I assembly in mammals (Guerrero-Castillo et al. 2017; Formosa et al. 2018). In land plants, four assembly factors are functionally characterized. The L-galactono-1,4-lactone dehydrogenase (GLDH) (Pineau et al. 2008; Schertl et al. 2012; Schimmeyer et al. 2016; Soufari et al. 2020) and CRK1 (Wang et al. 2022) participate in the assembly of the membrane arm. The protein INDH/NUBPL (Wydro et al. 2013) and the LYR protein CIAF1 (Ivanova et al. 2019) deliver Fe–S clusters to subunits of the matrix arm. INDH/NUBPL is also involved in mitochondrial translation (Wydro et al. 2013). Both INDH and CRK1 are conserved and have been functionally examined for their role in complex I assembly in mammals (Sheftel et al. 2009; Dunning et al. 2007), whereas GLDH and CIAF1 are plant-specific (Ivanova et al. 2019; Ligas et al. 2019).

Only two assembly factors have been functionally analyzed in *Chlamydomonas*. AMC1 is only found in *Chlamydomonas* and plays a role in the expression of the mitochondrial *nd4* gene (Subrahmanian et al. 2020), which encodes a core subunit of the P_d module. The absence of the assembly factor NDUFAF3 results in a lack of fully formed complex I in *Chlamydomonas* and a decrease in the abundance of some subunits of the Q module (Massoz et al. 2017). NDUFAF3 is conserved in plants and mammals. In humans, defects in NDUFAF3 are responsible for neonatal death and neurodevelopmental disorders and are characterized by a decreased abundance of Q module subunits. NDUFAF3 is required to join the Q and P modules (Saada et al. 2009; Ishiyama et al. 2018; Baertling et al. 2017; van der Ven et al. 2023; Guerrero-Castillo et al. 2017) and is proposed to work in association with NDUFAF4 (Guerrero-Castillo et al. 2017), an assembly factor present in land plants (Ligas et al. 2019), but absent in *Chlamydomonas* (Subrahmanian et al. 2016). Considering that NDUFAF3 is only functionally characterized in mammals and that NDUFAF4 is missing in *Chlamydomonas*, we decided to examine the role of NDUFAF3 in complex I assembly in *Chlamydomonas*.

Our analyses demonstrate the association of NDUFAF3 with an assembly intermediate containing subunits of the Q/P modules, along with additional complex I components not found in mammals and fungi such as the γ carbonic anhydrase domain and C1-FDX of the ferredoxin bridge. Structural predictions position NDUFAF3 at a stage preceding the consolidation of this bridge. Further analyses indicate that the N module is the last to be assembled, demonstrating that the mitochondrial complex I of *Chlamydomonas* follows a human-like construction pathway.

2 | Materials and Methods

2.1 | Strains and Culture Media

All strains were derived from the 137C strain from the *Chlamydomonas* collection. The *ndufaf3* mutant (Massoz et al. 2017), wild-type (Ct), and complemented strains isolated in

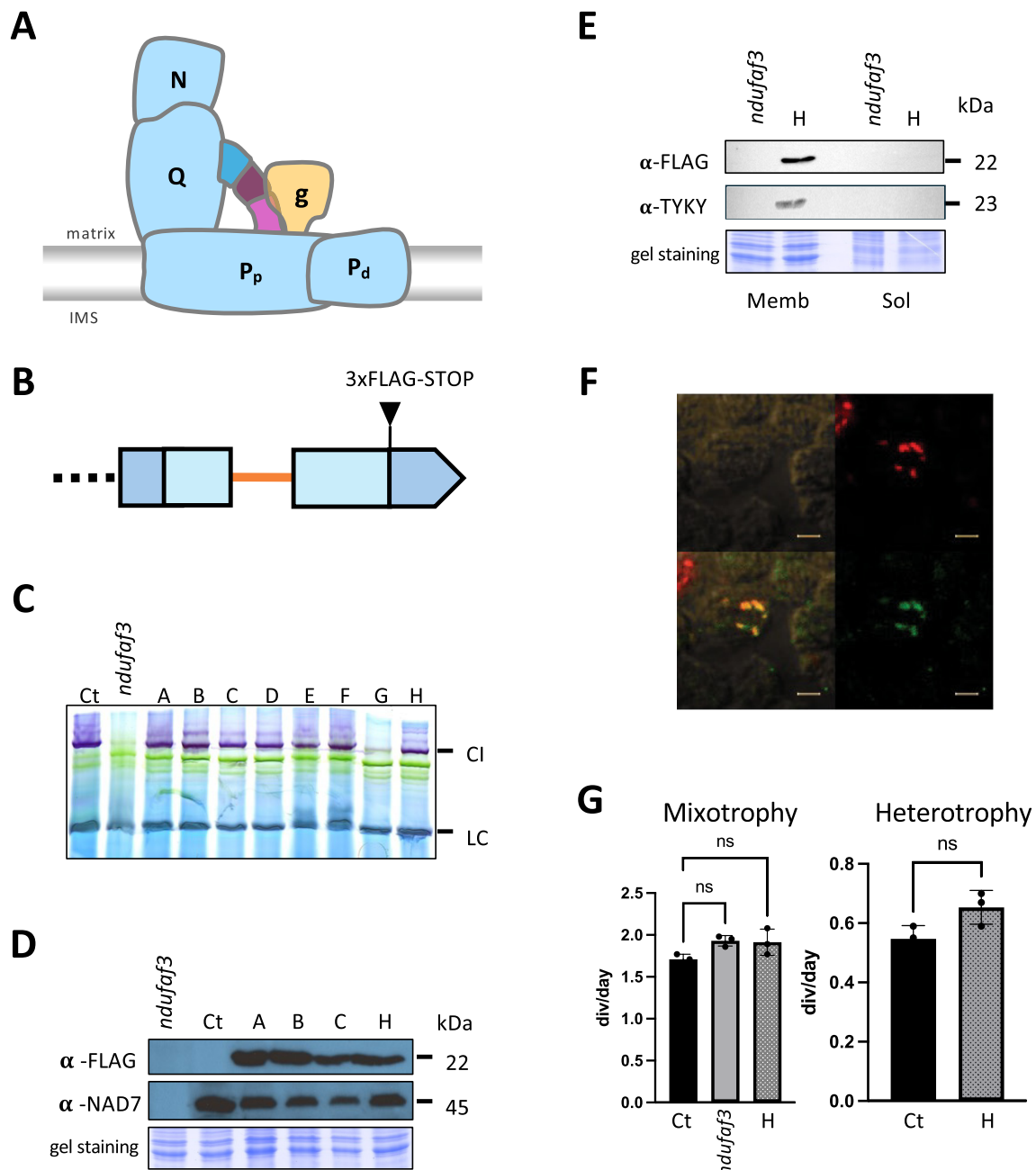


FIGURE 1 | The *NDUFAF3-3xFLAG* gene restores complex I activity in a *ndufaf3* mutant and its corresponding gene product is addressed to mitochondria. (A) Modular structure of complex I. Schematic representation of the complex I structure, including the ferredoxin bridge composed, from left to right, of the B14 (blue), SDAP (dark red), C1-FDX (pink), and γ carbonic anhydrase domain (yellow) subunits. The modules of the matrix arm (N and Q modules) and the membrane arm (P_p and P_d modules) are shown in blue. IMS: Intermembrane space. (B) Schematic representation of *NDUFAF3-3xFLAG* gene (Cre12.g496800) synthetic gene. Dark blue boxes represent endogenous 5' and 3' UTRs, whereas light blue boxes depict exons. The 3xFLAG tag insertion site is indicated by the black arrow. The orange line represents the *RBCS2i1* intron engineered in the construct, and the dotted grey line depicts the endogenous promoter (200bp) (see Figure S1 for details). (C) NADH/NBT staining of native protein complexes from membrane extracts of eight *NDUFAF3-3xFLAG*-expressing transformants (A–H), the recipient mutant (*ndufaf3*), and the wild-type (Control, Ct) strain (600 μ g of proteins per lane) separated by BN-PAGE. CI, complex I; LC, loading control. (D) Immunoblots of membrane fractions (20 μ g of proteins per lane) incubated with antibodies against the FLAG tag of *NDUFAF3-3xFLAG* and NAD7. A Coomassie blue-stained gel loaded with the same extracts is included as a loading control. (E) Immunoblots of membrane fractions (Memb: 20 μ g of proteins per lane) and soluble fractions (Sol: 20 μ g of proteins per lane) incubated with FLAG or TYKY antibodies. A Coomassie blue staining of a gel loaded with the same extracts is included as a loading control. (F) Immunofluorescence staining of fixed cells of the H transformant visualized by confocal microscopy: upper left: brightfield image; upper right: MitoTracker Orange staining; lower right: Alexa Fluor 488 conjugated FLAG-tag antibodies; lower left: merged image. Scale: 2 μ m. (G) Growth rates (number of divisions/24 h) in mixotrophy and heterotrophy. $n=3$, error bars are standard deviations, ns = non-significant. Statistical analysis was performed using Ordinary one-way ANOVA for growth in mixotrophy and an unpaired *t*-test for growth in heterotrophy.

this work were grown at 25°C under mixotrophic conditions in Tris-acetate phosphate (TAP) medium (Harris 1989) under continuous low light (50 $\mu\text{mol photons m}^{-2}\text{s}^{-1}$) or in heterotrophic conditions. Division rates in the exponential phase were measured according to (Pulich and Ward 1973).

2.2 | Transformation

Complementation experiments were performed as described in (Massoz et al. 2017), using the *ndufaf3* mutant as the recipient strain. The mutant was transformed with 5 μg of the pGH-NDUFAF3-3 \times FLAG plasmid (Figure S1) and 3 μg of the pSL18 plasmid containing the *aphVIII* gene encoding resistance to paromomycin (Depège et al. 2003). Transformants were selected on paromomycin (10 $\mu\text{g mL}^{-1}$) containing TAP medium. The pGH-NDUFAF3-3 \times FLAG construct was obtained by replacing a *PstI-XbaI* fragment of the untagged synthetic *NDUFAF3* gene described in (Massoz et al. 2017) with a fragment containing a 3 \times FLAG encoding sequence (GAC TAC AAG GAC CAC GAC GGT GAC TAC AAG GAC CAC GAC ATC GAC TAC AAG GAC GAC GAC GAC AAG) before the STOP codon (Figure S1). This construct was synthesized by IDT (<https://eu.idtdna.com/>).

2.3 | Biochemical Analyses

As described in (Remacle et al. 2001), membrane fractions were recovered by sonication and differential centrifugation. Soluble fractions were obtained by recovery of the supernatant of the membrane fractions. Purified mitochondria fractions were isolated from a cell wall-less strain, as described in (Cardol et al. 2002). Protein amounts were determined using the Bradford assay method (Bradford 1976). Immunoblotting was performed using standard protocols. Antibodies against TYKY (NUO8, Barbieri et al. 2011) and NAD1 (kind gift of E Meyer, Germany) were used at 1/3500 dilution; antibodies against NAD7 (NUO7, Barbieri et al. 2011) were used at 1/2000 dilution. Antibodies against the FLAG tag (Sigma-Aldrich) were used at 1/5000 dilution. Solubilization of crude membrane and mitochondria-enriched fractions using *n*-dodecyl- β -D-maltoside (1.7% w/v), BN-PAGE (4%–15% pre-cast gradient gels, Bio-Rad), and the subsequent staining of the gel by NADH/NBT (nitroblue tetrazolium) were done as previously published (Cardol et al. 2002).

For 2D-BN/SDS PAGE, BN gels were sliced in between each well (150–200 μg of solubilized mitochondria per well) and incubated in 2 \times Laemmli buffer for 45 min before being transferred to a 15% polyacrylamide (with 4% stacking gel) SDS gel. The second dimension SDS gels were run at 180 V for ~1 h at 4°C in buffer (0.25 M Tris-HCl pH 8.3, 0.192 M glycine, 0.1% SDS). Immunoblotting was performed using standard protocols and the same antibody dilutions listed above. Images were aligned based on complex I and complex I subunit signaling location and gel/blot size.

The molecular masses of the two species detected by the FLAG antibodies in the 2D BN-SDS PAGE were estimated based on their migration distances, using the respiratory complexes as

size references (the linear regression between the logarithm of the molecular mass (kDa) and the migration distance of the respiration complexes has a R^2 of 0.99).

2.4 | Co-Immunoprecipitations

Immunoprecipitations were conducted using purified mitochondria corresponding to 0.5–1 mg of protein with the μMACS DYKDDDDK (FLAG) or Protein G Isolation Kits (Miltenyi Biotec), following the methodology of (Waltz et al. 2019). The immunoprecipitations with DYKDDDDK (FLAG) beads involved purified mitochondria from the NDUFAF3-3 \times FLAG-tagged strain compared to those from the wild-type strain. Immunoprecipitations using Protein G beads were carried out in the presence or absence (as control) of 2.5 μg of TYKY antibodies with purified mitochondria from the NDUFAF3-3 \times FLAG-tagged strain. Purified mitochondria were lysed using a lysis buffer composed of 20 mM HEPES-KOH (pH 7.6), 100 mM KCl, 30 mM MgCl_2 , 1 mM DTT, 0.3% *n*-dodecyl- β -D-maltoside (v/v), and 1% Triton X-100 (v/v), supplemented with protease inhibitors (cOmplete, EDTA-free protease inhibitor cocktail, Roche). Washing steps were performed with a wash buffer similar to the lysis buffer described above, but containing 0.01% *n*-dodecyl- β -D-maltoside and 0.1% Triton X-100 (v/v).

Mass spectrometric analyses were conducted at the Strasbourg-Esplanade Proteomics Facility (<https://ibmc.cnrs.fr/en/laboratoire/mass-spectrometry/equipes/strasbourg-esplanade-proteomics-facility/>). Eluted proteins from the immunoprecipitated samples were reduced (5 mM DTT), alkylated (10 mM iodoacetamide) and digested with 300 ng trypsin. Generated peptides were analyzed by nanoLC-MS/MS on a reversed-phase nanoE-lute 2 coupled to a TIMS-TOF Pro 2 mass spectrometer (Bruker Daltonik GmbH) using a data-dependent acquisition (DDA). Peptides were separated on an IonOpticks Aurora Elite column (25 cm \times 75 μm , 1.7 μm particle size and 120 Å pore size; AUR3-15075C18-CSI) with 70 min gradients. Data were searched against the *Chlamydomonas reinhardtii* CC-4532 v6.1 annotated genome (Phytozome v13) using Mascot (Matrix Science, v2.8). Proteins were then validated in Proline (ProFI) with an FDR < 1% (false discovery rate) at both Peptide Spectrum Mass (PSM) and protein levels, and a PSM score > 25. Statistical analysis of the immunoprecipitation data from three biological replicates was conducted using Extract Ion Chromatogram (peptides intensities) (XIC) abundance using the R software package (<https://github.com/hzuber67/IPinquiry4>). The data have been deposited on the PRIDE platform.

2.5 | Confocal Microscopy

Fixed *Chlamydomonas* cell imaging was performed on a Leica TCS SP5 inverted confocal laser microscope (Leica Microsystems). Images were collected using a water-immersion objective at 512 \times 512 pixel resolution. Alexa Fluor 488 conjugated FLAG-tag antibodies (ThermoFisher Scientific) were visualized using the 488 nm line of the argon laser, and the emission light was dispersed and recorded at 495–532 nm (for an optimized detection at 525 nm). MitoTracker Orange (ThermoFisher Scientific) was visualized using the HeNe 543 nm laser, and the

emission light was dispersed and recorded at 564–602 nm (for an optimized detection at 576 nm).

2.6 | Structural Modeling

Complex I subunits and NDUFAF3 structures and interactions were predicted using version/release 2.2.0 of the software AlphaFold2. Predictions were performed and run locally using our in-house computer cluster (Jumper et al. 2021). For the prediction, the hypothesized mitochondrial targeting sequences (MTS) were trimmed from the sequences. Figures featuring atomic models were visualized with UCSF ChimeraX (Pettersen et al. 2021). The complex I subunits were colored according to $-\log_{10}$ (adjusted p value) by creating a custom attribute assignment file in ChimeraX.

2.7 | Accession Numbers

Raw proteomic data have been deposited on the PRIDE platform (Project PXD048077).

3 | Results

3.1 | NDUFAF3-3×FLAG Restores Complex I Assembly in Complemented *ndufaf3* Strains

To examine the role of NDUFAF3 in complex I assembly, we generated an algal strain bearing a tagged version of *NDUFAF3*. To achieve this, we transformed a previously characterized *ndufaf3* mutant (Massoz et al. 2017) with a resistance cassette to paromomycin and a construct encoding a 3×FLAG-tag at the C-terminus of NDUFAF3 (see experimental procedures for details) (Figures 1B and S1). The non-tagged version of this construct has been successfully used to complement the *ndufaf3* mutant (Massoz et al. 2017). Complex I was detected in eight paromomycin-resistant transformants (A–H) by NADH/NBT staining after separating native protein complexes from membrane extracts via BN-PAGE. A wild-type strain (Ct) and the *ndufaf3* mutant were used as positive and negative controls, respectively. The transformants showed restored NADH dehydrogenase activity and assembly of complex I and could not be distinguished from the wild type except for clone G (Figure 1C). Among them, four transformants (A, B, C, H) were chosen for further analysis. The presence of the FLAG epitope of NDUFAF3 was verified by immunoblotting after separation of membrane extracts by SDS-PAGE (Figure 1D). Figure 1D also shows that the NAD7 subunit of the Q module is detected in all these transformants, like in Ct, but not in the *ndufaf3* mutant, as already reported in *Chlamydomonas* and humans (Massoz et al. 2017; Baertling et al. 2017; Ishiyama et al. 2018). The H transformant was chosen for further analyses. Since the Q module is part of the hydrophilic arm, we asked if NDUFAF3 could be detected in a soluble extract. As shown in Figure 1E, the signal related to NDUFAF3 is detected in the membrane fraction of the H transformant and not in the soluble fraction. It can thus be hypothesized that NDUFAF3 is associated with membrane-anchored intermediate modules in complex I assembly. The same result is obtained for the TYKY subunit of the Q module.

Immunofluorescence staining of type H transformant cells with a probe to detect mitochondria (MitoTracker) and the FLAG epitope of NDUFAF3 (with Alexa Fluor 488) is shown in Figure 1F. The yellow color in the merged image illustrates the colocalization of the fluorescent signals identifying mitochondria and NDUFAF3 (Figure 1F). We concluded that the tagged subunit is indeed localized in mitochondria. At last, the growth rate of the H transformant is the same as that of the Ct strain in light (light + acetate, mixotrophy) and dark (dark + acetate, heterotrophy) conditions (Figure 1G). In contrast, the growth of the *ndufaf3* mutant is null in heterotrophic conditions (not presented on the graph). Together, these results indicate that the *NDUFAF3-3×FLAG* gene copy present in the H transformant restores the respiratory capacity when expressed in the *ndufaf3* mutant.

3.2 | NDUFAF3-3×FLAG-Tagged Is Detected in Two Assembly Intermediates by Immunodetection Analysis

To detect complex I assembly intermediates associated with NDUFAF3-3×FLAG, native protein complexes from membrane extracts of the Ct strain and the H transformant were separated by BN-PAGE, followed by immunoblotting analysis. When the anti-FLAG antibodies were used, two subcomplexes were detected in the H transformant. The size of these subcomplexes is smaller than the whole complex I, revealed by NADH/NBT staining (Figure 2A). As a control, anti-TYKY antibodies were also used since this subunit belongs to the Q module, which is known to interact with NDUFAF3 (Guerrero-Castillo et al. 2017). A signal corresponding to whole complex I is detected with the anti-TYKY antibodies for the Ct strain and the H transformant, confirming the integrity of complex I in the complemented strain (Figure 2B). No signal is detected in membrane extracts of the *ndufaf3* mutant since this subunit of the Q module is not accumulated in this mutant (Massoz et al. 2017), like NAD7 (Figure 1D).

Since the signals detected using the anti-FLAG antibodies were noisy on membrane fractions, mitochondria were isolated from the strain expressing the *NDUFAF3-3×FLAG* construct (H transformant) and two-dimensional BN-SDS-PAGE (2D BN/SDS-PAGE) followed by immunoblotting analysis using specific antibodies was performed on mitochondrial extracts (Figure 2C). Two protein complexes are recognized by the FLAG antibodies, with an apparent molecular mass of approximately 700 and 500 kDa, based on the migration pattern of the respiratory complexes (see the experimental procedure for details). These findings are in agreement with the results obtained in Figure 2A. In addition, a smear is found both below and above these two main spots. Distinct signals revealing the presence of NAD7 and TYKY align with in-gel staining for complex I activity, indicating the presence of these subunits in the holoenzyme, as expected from results obtained on the membrane fraction (Figure 2B). NAD7 and TYKY are also immunodetected below and above complex I, at a higher molecular weight, also stained in the NBT gel, which corresponds to the documented supercomplex I+III₂ (Cardol et al. 2006, 2008; Waltz et al. 2025). Considering the two main spots detected using the anti-FLAG antibodies, these results suggest that NDUFAF3 is probably transiently associated with two intermediates of complex I,

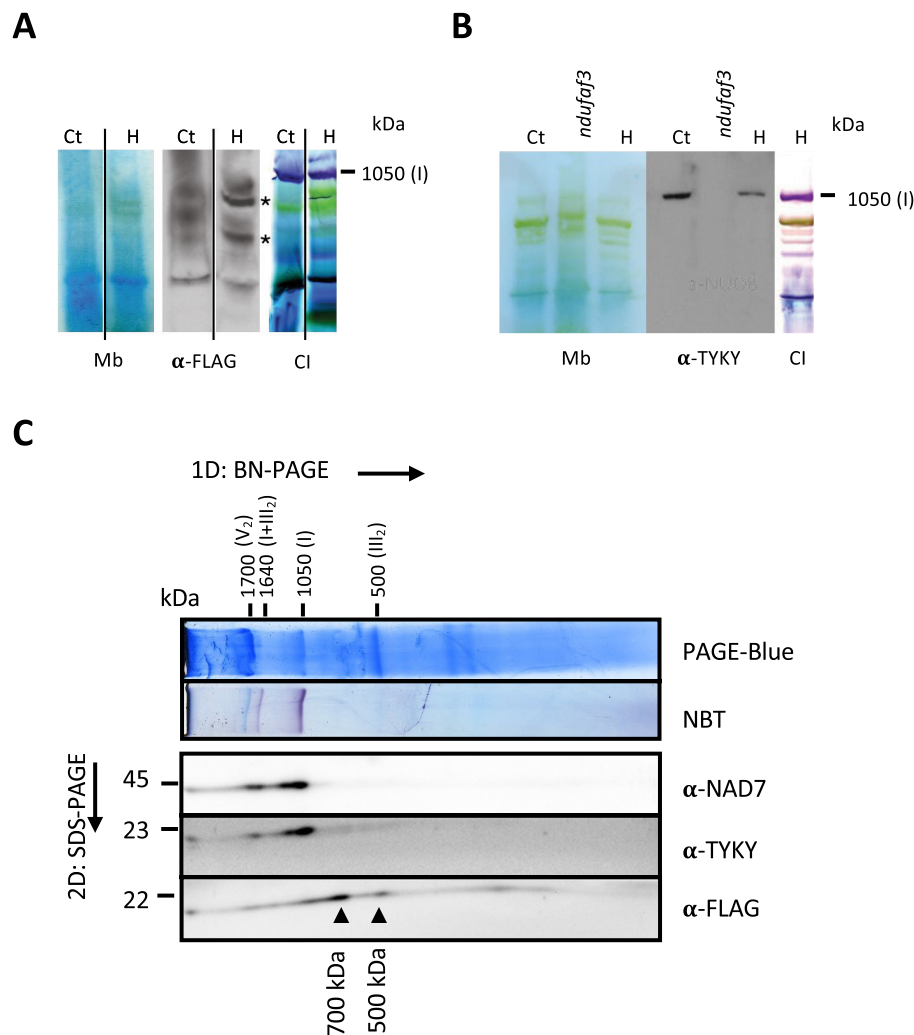


FIGURE 2 | Analysis of complex I assembly by 2D BN/SDS PAGE reveals that NDUFAF3 co-migrates with two intermediates. (A) Membrane extracts from control (Ct) and H strain were resolved in native conditions (BN-PAGE). The left part (Mb) represents the blotted membrane before incubation with antibodies against the FLAG tag of NDUFAF3 (α -FLAG), the middle panel represents the immunoblot, and the right panel (CI) represents NADH staining for complex I activity. The asterisks indicate the position of the NDUFAF3 containing complexes (~700 and 500 kDa). The black lines indicate the separation on the membrane/blot/gel between the loadings of Ct and H transformant, signifying some samples unrelated to the study. (B) Membrane extracts from control (Ct), *ndufaf3* and H strain were resolved in native conditions (BN-PAGE). The left part (Mb) represents the blotted membrane before incubation with antibodies against the TYKY antibodies, the middle panel represents the immunoblot, the right panel (CI) represents NADH staining for complex I activity. (C) Purified mitochondria samples were resolved in native conditions (left to right) and denaturing conditions (top to bottom). Starting at the top, the panels display an enriched mitochondrial fraction, NADH/NBT staining of the mitochondrial fraction, and immunoblots against the NAD7 and TYKY complex I subunits and the FLAG tag of NDUFAF3. V_2 , I + III₂, I, and III₂, correspond to respiratory chain complexes V (dimeric state), supercomplex I + III₂, complex I, and complex III (dimeric state), respectively (Cardol et al. 2006, 2008; Waltz et al. 2025). The grey arrows identify the position of the NDUFAF3 containing complexes (~700 and 500 kDa).

although we do not have confirmation that they are bona fide complex I assembly submodules.

3.3 | Physical Interaction of NDUFAF3-3 \times FLAG-Tagged With Subunits Specific to the Q, P_p, and P_d Modules

Co-immunoprecipitation analysis was performed to confirm the physical interactions of NDUFAF3 with complex I subunits. Purified mitochondrial solubilized extracts from the H transformant expressing NDUFAF3-3 \times FLAG-tagged were immunoprecipitated with anti-FLAG antibodies, and subsequent elutions

were analyzed by nanoLC-MS/MS. We also conducted the co-immunoprecipitation experiment with a wild-type strain (Ct) as a negative control. Three biological replicates were prepared for both strains (NDUFAF3-3 \times FLAG-tagged and Ct). Analysis showed that 119 proteins were statistically relevant with an adjusted p value < 0.05 . Among them, 35 subunits of complex I were found: 27 presented a $\text{Log}_2\text{FC} > 3$, while 8 were below this threshold. Since two subunits presenting a $\text{Log}_2\text{FC} < 3$ (the 75 kDa subunit $\text{Log}_2\text{FC} = 2.39$ and Nad1 $\text{Log}_2\text{FC} = 2.43$) were detected on membrane extracts of the *ndufaf3* mutant (Massoz et al. 2017 and Figure S2), this suggested that interactions with NDUFAF3 were weak below $\text{Log}_2\text{FC} = 3$. For the 52 proteins with a $\text{Log}_2\text{FC} > 3$, a functional enrichment analysis confirmed

that “mitochondrial respiratory chain complex I” was by far the most enriched cellular component using anti-FLAG antibodies (Figure S3A). This led us to conclude that NDUFAF3 mostly interacts with complex I subunits and to consider the 27 complex I subunits with $\text{Log}_2\text{FC} > 3$ as potential interactors of NDUFAF3.

NDUFAF3-3×FLAG-tagged is the fifth most enriched protein with a $\text{Log}_2\text{FC}=5.84$ (Figure 3A, Table S6). This is expected since NDUFAF3 was the bait used for this analysis. The subunits identified belong mostly to the Q, P_p , and P_d modules (Figure 3B). Included are several protist and plant subunits not found in mammals and fungi complex I: the three γ carbonic anhydrase subunits (CAG1-3), of which CAG3 is the strongest interactant with NDUFAF3, C1-FDX (NUOP3 in *Chlamydomonas*) of the ferredoxin bridge, P1 (NUOP5, in *Chlamydomonas*), NUOP7, and P9 (Cardol et al. 2004; Klusch et al. 2021) (Figure 3A,B, Table S6). Only one subunit of the N module was detected with a $\text{Log}_2\text{FC} > 3$, the 18 kDa subunit, which forms contacts between the N and the Q modules (Waltz et al. 2025). By summing the molecular masses of the detected proteins, the expected size of the module is 579 kDa (Table S7), which is in the range of the sizes of the two complexes identified by 2D BN/SDS-PAGE (500 and 700 kDa) (Figure 2C). In conclusion, these findings demonstrate that NDUFAF3 is present in a large subcomplex, comprising subunits of both the hydrophilic and hydrophobic arms of complex I, with strong interactions with the Q module and the carbonic anhydrase domain.

3.4 | The N Module Is the Last to Be Assembled in *Chlamydomonas* Complex I

Except the 18 kDa subunit, the other subunits of the N module co-immunoprecipitated with NDUFAF3 are only loosely attached to the complex I subassembly detected ($\text{Log}_2\text{FC}=2.39$ for the 75 kDa

subunit, 1.75 for the 24 kDa subunit, 1.70 for the 51 kDa subunit, 1.53 for the 13 kDa subunit, Table S6). This suggests that the N module is the last one to join complex I, after the association between the Q and P modules. This contrasts with the situation in Angiosperms where the N and Q modules join before their anchoring to the membrane. A co-immunoprecipitation with antibodies against a subunit of the Q module, the TYKY subunit, was thus performed on solubilized mitochondria of the H transformant to determine which type of subassembly (N/Q, or NQP) could be captured. As expected, immunoprecipitation data showed that TYKY was the most enriched protein ($\text{Log}_2\text{FC}=7.68$) (Figure S4). A functional enrichment on the 167 statistically relevant proteins with a $\text{Log}_2\text{FC} > 3$ showed that the cellular component “mitochondrial respiratory chain complex I” was also the most enriched, like for the co-immunoprecipitation with anti-FLAG antibodies, demonstrating the specificity of the anti-TYKY antibodies toward complex I subunits (Figure S3B). Results also showed that the subunits of the N module are indeed much more enriched compared to the co-immunoprecipitation with anti-FLAG antibodies (NDUFAF3), together with subunits of the Q, P_p , and P_d modules (Figures 4 and S4; Table S8). Thirty-eight subunits (against 27 when co-immunoprecipitation is performed with anti-FLAG antibodies) were detected using the same threshold of $\text{Log}_2\text{FC} > 3$, which suggests that a nearly mature form of complex I has been captured for a size of 858 kDa (Table S7), close to the 1050 kDa of the mature complex I. These findings agree with the hypothesis that the N module is attached at a late assembly stage, when the Q, P_p , and P_d modules are already joined together.

4 | Discussion

NDUFAF3 is one of the seven assembly factors (NDUFAF2-7, INDH/NUBPL) responsible for assembling the matrix arm of

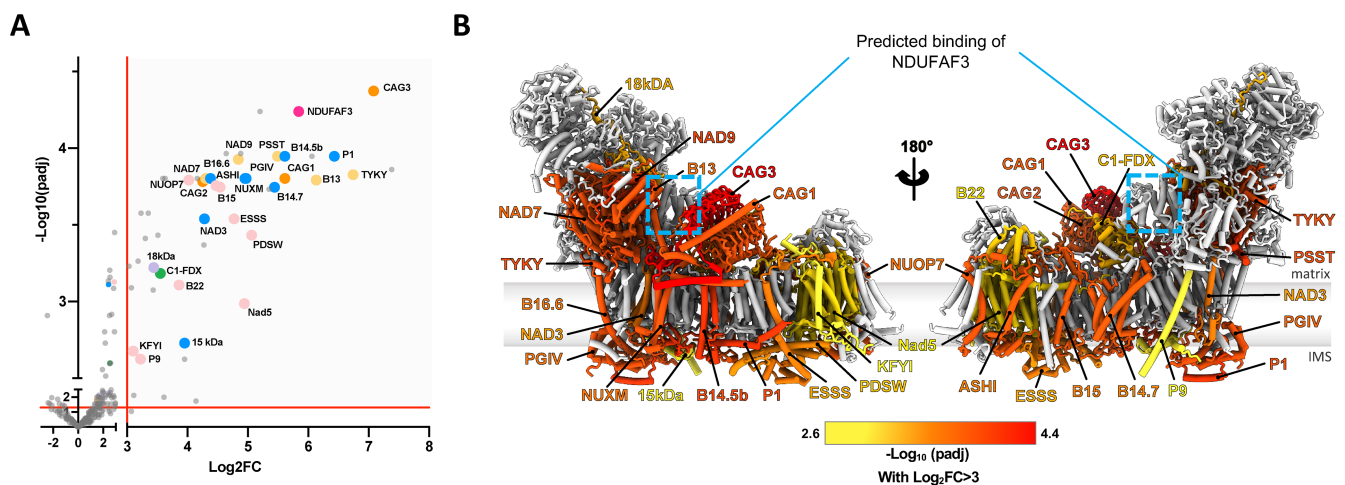


FIGURE 3 | NDUFAF3 is associated with subunits of the Q and P modules, including plant-specific proteins. (A) Volcano plot illustrating the global enrichment of proteins in the immunoprecipitation of NDUFAF3-3×FLAG-tagged versus the control strain ($n=3$). The x-axis represents the Log_2 fold change (Log_2FC), whereas the y-axis displays $-\text{Log}_{10}$ of the adjusted p value ($-\text{Log}_{10}[\text{adj}]$), obtained using the IPInquiry4 R software package. Significantly enriched proteins are defined by a $\text{Log}_2\text{FC} > 3$ and a $-\text{Log}_{10}(p\text{-adj}) > 1.3$ (corresponding to an adjusted p value < 0.05), as indicated by the red axes. NDUFAF3 is marked by a red dot; the N module subunits are shown in violet, the Q module subunits in yellow, the P_p module subunits in blue, the P_d module subunits in pink, the ferredoxin bridge subunits in green, and the γ carbonic anhydrase subunits in orange. The complete datasets and analyses are available in the supplemental (Table S6). (B) Structural model of mitochondrial complex I from *Chlamydomonas* (Waltz et al. 2025). IMS, intermembrane space. The subunits with a $\text{Log}_2\text{FC} > 3$ are colored according to $-\text{Log}_{10}(p\text{-adj})$. The predicted binding region from the AlphaFold2 multimer is shown by dashed blue squares. The AlphaFold prediction is available in the supplemental (Figure S5).

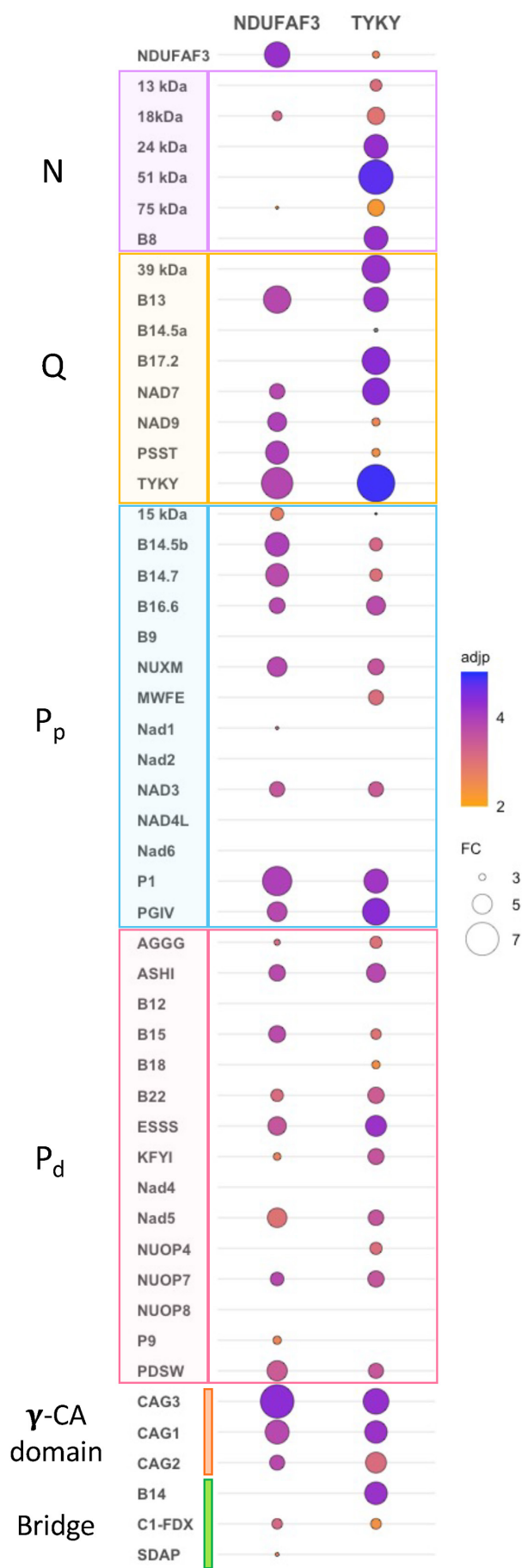


FIGURE 4 | Comparison of NDUFAF3 and TYKY co-immunoprecipitation experiments. Balloon plots illustrate the NDUFAF3 and TYKY co-immunoprecipitation results. The area of each balloon represents the enrichment in Log₂ fold change (FC) of the two co-immunoprecipitations relative to the various subunits of complex I, while the color gradient indicates the -Log₁₀ of the adjusted *p* value (adj). The fold change (FC) and adjusted *p* value (adj) cut-offs are indicated. The different modules of complex I are identified according to the color code in Figure 3A.

complex I in humans and conserved in plants (Guerrero-Castillo et al. 2017; Ligas et al. 2019). However, NDUFAF3 was not found to be associated with complex I modules in Arabidopsis, which prevented the assessment of its role in the assembly process (Ligas et al. 2019). In addition, NDUFAF3 is encoded by two isoforms in Arabidopsis (At3g60150/At2g44525), which suggests possible redundancy (Ligas et al. 2019). To further elucidate the steps of complex I assembly, we constructed a strain with a functional flagged NDUFAF3 in *Chlamydomonas*. The physical association of NDUFAF3 with a complex I intermediate could be demonstrated by co-immunoprecipitation followed by nanoLC-MS/MS analysis of detergent-solubilized mitochondria from the NDUFAF3-3×FLAG expressing strain. According to the assembly pathway of human complex I proposed by Guerrero et al., NDUFAF3 is present at multiple stages of the assembly process (Guerrero-Castillo et al. 2017). Its association with complex I subassemblies starts with a soluble form of the Q module and remains until the Q module is attached to the P_p and the P_d module (Guerrero-Castillo et al. 2017). The data presented here show that the co-immunoprecipitation using the anti-FLAG antibodies has captured a late stage of NDUFAF3-associated subassembly, where the Q, P_p, and P_d modules are joined together. In addition, our results suggest that NDUFAF3 joins the assembly when the Q module is already attached to the inner mitochondrial membrane, since NDUFAF3 is only recovered in membrane extracts by immunodetection. This is not surprising since it has recently been demonstrated (Sung et al. 2024) that in humans the Q module attaches to the inner mitochondrial membrane earlier than was previously suggested in the model of (Guerrero-Castillo et al. 2017). Our findings also show that subunits present in plant, algal, and protist complex I but not in mammal and fungi complex I (Braun and Klusch 2024) are present in the subassembly intermediate associated with NDUFAF3 in *Chlamydomonas*.

The superimposition of the subunits detected by co-immunoprecipitation with anti-FLAG antibodies within complex I highlights that NDUFAF3 interacts strongly with subunits of the Q and P modules (Figure 3B), which is expected based on the role of NDUFAF3 (Guerrero-Castillo et al. 2017). Using AlphaFold2 multimer (Jumper et al. 2021), a structural model of NDUFAF3 in association with Q module subunits (NAD7, 9, TYKY, PSST, B13) was generated (Figure S5). The structural prediction of association is strong (pLDDT score > 90, Figure S5C), confirming the essential role of NDUFAF3 in the assembly of key subunits of the Q module, as already proposed (Guerrero-Castillo et al. 2017). Moreover, the predicted positioning of NDUFAF3 within the Q module reveals a potential steric hindrance with the B14 and SDAP subunits, which belong to the

ferredoxin bridge, in addition to C1-FDX (Klusck et al. 2021). As mentioned above, C1-FDX was identified as an interactor of NDUFAF3 via the co-immunoprecipitation experiments, whereas B14 was not detected and SDAP was below the threshold of $\text{Log}_2\text{FC} = 3$ (Table S6), which explains the partial enrichment of the ferredoxin bridge on Figure 3B. Given the context of the position of NDUFAF3 at the level of the Q module, the structural prediction suggests that NDUFAF3 plays a role in finalizing the assembly of the ferredoxin bridge, likely present in the Last Eukaryotic Common ancestor (LECA) (Braun and Klusck 2024).

Of note is the presence of the 18 kDa subunit of the N module in the subassembly complex detected with anti-FLAG antibodies. This subunit is proposed to stabilize the N module in mammalian complex I (Yin et al. 2024). The presence of this subunit suggests that the subassembly captured with the anti-FLAG antibodies is at a stage where the N module starts to be assembled. This would explain why the NDUFAF2 assembly factor, which is binding to the Q module and prevents the joining of the N module (Guerrero-Castillo et al. 2017) is not found in the co-immunoprecipitation. The other subunits of the N module are below the threshold when probing for interactions with NDUFAF3-3 \times FLAG, but are well detected together with subunits of the Q, P_p, and P_d modules when co-immunoprecipitation is performed with TYKY antibodies. This demonstrates that the N module is attached at the last stage of complex I assembly, like in mammalian and fungal complex I. In Angiosperms, the entire matrix arm (N and Q modules) is formed before the addition of the membrane arm (Ligas et al. 2019; López-López et al. 2022).

In the assembly of human complex I, NDUFAF3 is associated with NDUFAF4 (Guerrero-Castillo et al. 2017). In the fruit fly, overexpression of *NDUFAF4* can partially overcome some NDUFAF3 defects (Murari et al. 2021), indicating functional redundancy between the two assembly factors. The absence of NDUFAF4 and the existence of only one isoform of *NDUFAF3* in *Chlamydomonas*, contrary to Arabidopsis, is unclear. One interpretation is that complex I assembly in *Chlamydomonas* is simple, and this could reflect the basal phylogenetic position of this microalga in eukaryotes.

In conclusion, these results underscore the uniqueness of *Chlamydomonas* for the study of complex I manufacture in non-mammalian systems.

Author Contributions

T.S.-G. designed and performed the experiments. M.T., F.W., N.C., S.F., J.C., P.H. performed the experiments. T.S.-G., M.T., N.C., S.F., J.C., P.H., P.P.H., C.R. analyzed the data. C.R. designed and conducted the experiments and wrote the initial version of the manuscript. T.S.-G., M.T., F.W., and P.P.H. reviewed the manuscript, and all authors approved the final version.

Acknowledgments

In memory of Dr. S. Massoz, who died at Age 34 and pioneered this research. M. Radoux is acknowledged for technical support. Dr. E. Meyer (Martin-Luther-University Halle-Wittenberg, Germany) is acknowledged for the kind gift of the antibodies against Arabidopsis Nad1. We thank G. Herinckx and Dr. D. Vertommen from UCLouvain (Belgium)

for the pilot proteomics experiments done on BN-PAGE. We thank V. Cognat from the IBMP bioinformatics core facility for her assistance with the protein functional analyses.

Data Availability Statement

Raw proteomic data have been deposited on the PRIDE platform (Project PXD048077).

References

- Baertling, F., L. Sánchez-Caballero, S. Timal, et al. 2017. "Mutations in Mitochondrial Complex I Assembly Factor NDUFAF3 Cause Leigh Syndrome." *Molecular Genetics and Metabolism* 20: 243–246.
- Barbieri, M. R., V. Larosa, C. Nouet, N. Subrahmanian, C. Remacle, and P. P. Hamel. 2011. "A Forward Genetic Screen Identifies Mutants Deficient for Mitochondrial Complex I Assembly in *Chlamydomonas reinhardtii*." *Genetics* 188: 349–358.
- Bradford, M. M. 1976. "A Rapid and Sensitive Method for the Quantitation of Microgram Quantities of Protein Utilizing the Principle of Protein-Dye Binding." *Analytical Biochemistry* 72: 248–254.
- Braun, H.-P., and N. Klusck. 2024. "Promotion of Oxidative Phosphorylation by Complex I-Anchored Carbonic Anhydrases?" *Trends in Plant Science* 29: 64–71.
- Cardol, P., L. Boutaffala, S. Memmi, B. Devreese, R. F. Matagne, and C. Remacle. 2008. "In *Chlamydomonas*, the Loss of ND5 Subunit Prevents the Assembly of Whole Mitochondrial Complex I and Leads to the Formation of a Low Abundant 700 kDa Subcomplex." *Biochimica et Biophysica Acta* 1777: 388–396.
- Cardol, P., M. Lapaille, P. Minet, F. Franck, R. F. Matagne, and C. Remacle. 2006. "ND3 and ND4L Subunits of Mitochondrial Complex I, Both Nucleus Encoded in *Chlamydomonas reinhardtii*, Are Required for Activity and Assembly of the Enzyme." *Eukaryotic Cell* 5: 1460–1467. <https://doi.org/10.1128/EC.00118-06>.
- Cardol, P., R. F. Matagne, and C. Remacle. 2002. "Impact of Mutations Affecting ND Mitochondria-Encoded Subunits on the Activity and Assembly of Complex I in *Chlamydomonas*. Implication for the Structural Organization of the Enzyme." *Journal of Molecular Biology* 319: 1211–1221.
- Cardol, P., F. Vanrobaeys, B. Devreese, J. Van Beeumen, R. F. Matagne, and C. Remacle. 2004. "Higher Plant-Like Subunit Composition of Mitochondrial Complex I From *Chlamydomonas reinhardtii*: 31 Conserved Components Among Eukaryotes." *Biochimica et Biophysica Acta* 1658: 212–224.
- Depège, N., S. Bellafiore, and J.-D. Rochaix. 2003. "Role of Chloroplast Protein Kinase Stt7 in LHCII Phosphorylation and State Transition in *Chlamydomonas*." *Science* 299: 1572–1575.
- Dudkina, N. V., S. Sunderhaus, E. J. Boekema, and H.-P. Braun. 2008. "The Higher Level of Organization of the Oxidative Phosphorylation System: Mitochondrial Supercomplexes." *Journal of Bioenergetics and Biomembranes* 40: 419–424.
- Dunning, C. J. R., M. McKenzie, C. Sugiana, et al. 2007. "Human CIA30 Is Involved in the Early Assembly of Mitochondrial Complex I and Mutations in Its Gene Cause Disease." *EMBO Journal* 26: 3227–3237.
- Formosa, L. E., M. G. Dibley, D. A. Stroud, and M. T. Ryan. 2018. "Building a Complex Complex: Assembly of Mitochondrial Respiratory Chain Complex I." *Seminars in Cell & Developmental Biology* 76: 154–162.
- Fromm, S., H. P. Braun, and C. Peterhansel. 2016. "Mitochondrial Gamma Carbonic Anhydrases Are Required for Complex I Assembly and Plant Reproductive Development." *New Phytologist* 211: 194–207.
- Galemou Yoga, E., H. Angerer, K. Parey, and V. Zickermann. 2020. "Respiratory Complex I—Mechanistic Insights and Advances in

- Structure Determination." *Biochimica et Biophysica Acta, Bioenergetics* 1861: 148153.
- Guerrero-Castillo, S., F. Baertling, D. Kownatzki, et al. 2017. "The Assembly Pathway of Mitochondrial Respiratory Chain Complex I." *Cell Metabolism* 25: 128–139.
- Harris, E. H. 1989. *The Chlamydomonas Sourcebook: A Comprehensive Guide to Biology and Laboratory Use*. Academic Press.
- Ishiyama, A., K. Muramatsu, S. Uchino, et al. 2018. "NDUFAF3 Variants That Disrupt Mitochondrial Complex I Assembly May Associate With Cavitating Leukoencephalopathy." *Clinical Genetics* 93: 1103–1106.
- Ivanova, A., M. Gill-Hille, S. Huang, et al. 2019. "A Mitochondrial LYR Protein Is Required for Complex I Assembly." *Plant Physiology* 181: 1632–1650.
- Jumper, J., R. Evans, A. Pritzel, et al. 2021. "Highly Accurate Protein Structure Prediction With AlphaFold." *Nature* 596: 583–589.
- Kampjut, D., and L. A. Sazanov. 2020. "The Coupling Mechanism of Mammalian Respiratory Complex I." *Science* 370: eabc4209.
- Klusch, N., J. Senkler, Ö. Yildiz, W. Kühlbrandt, and H.-P. Braun. 2021. "A Ferredoxin Bridge Connects the Two Arms of Plant Mitochondrial Complex I." *Plant Cell* 33: 2072–2091.
- Ligas, J., E. Pineau, R. Bock, M. A. Huynen, and E. H. Meyer. 2019. "The Assembly Pathway of Complex I in *Arabidopsis thaliana*." *Plant Journal* 97: 447–459.
- López-López, A., O. Keech, and N. Rouhier. 2022. "Maturation and Assembly of Iron-Sulfur Cluster-Containing Subunits in the Mitochondrial Complex I From Plants." *Frontiers in Plant Science* 13: 916948.
- Massoz, S., M. Hanikenne, B. Bailleul, et al. 2017. "In Vivo Chlorophyll Fluorescence Screening Allows the Isolation of a *Chlamydomonas* Mutant Defective for NDUFAF3, an Assembly Factor Involved in Mitochondrial Complex I Assembly." *Plant Journal* 92: 584–595. <https://doi.org/10.1111/tjp.13677>.
- Mühleip, A., R. K. Flygaard, R. Baradaran, et al. 2023. "Structural Basis of Mitochondrial Membrane Bending by the I-II-III-IV2 Supercomplex." *Nature* 615: 934–938.
- Murari, A., S.-K. Rhooms, C. Garcia, et al. 2021. "Dissecting the Concordant and Disparate Roles of NDUFAF3 and NDUFAF4 in Mitochondrial Complex I Biogenesis." *iScience* 24: 102869.
- Perales, M., G. Parisi, M. S. Fornasari, et al. 2004. "Gamma Carbonic Anhydrase Like Complex Interact With Plant Mitochondrial Complex I." *Plant Molecular Biology* 56: 947–957.
- Pettersen, E. F., T. D. Goddard, C. C. Huang, et al. 2021. "UCSF ChimeraX: Structure Visualization for Researchers, Educators, and Developers." *Protein Science* 30: 70–82.
- Pineau, B., O. Layoune, A. Danon, and R. De Paepe. 2008. "L-Galactono-1,4-Lactone Dehydrogenase Is Required for the Accumulation of Plant Respiratory Complex I." *Journal of Biological Chemistry* 283: 32500–32505.
- Pulich, W. M., and C. H. Ward. 1973. "Physiology and Ultrastructure of an Oxygen-Resistant *Chlorella* Mutant Under Heterotrophic Conditions." *Plant Physiology* 51: 337–344.
- Remacle, C., D. Baurain, P. Cardol, and R. F. Matagne. 2001. "Mutants of *Chlamydomonas reinhardtii* Deficient in Mitochondrial Complex I: Characterization of Two Mutations Affecting the nd1 Coding Sequence." *Genetics* 158: 1051–1060.
- Saada, A., R. O. Vogel, S. J. Hoefs, et al. 2009. "Mutations in NDUFAF3 (C3ORF60), Encoding an NDUFAF4 (C6ORF66)-Interacting Complex I Assembly Protein, Cause Fatal Neonatal Mitochondrial Disease." *American Journal of Human Genetics* 84: 718–727.
- Schertl, P., S. Sunderhaus, J. Klodmann, G. E. G. Grozeff, C. G. Bartoli, and H.-P. Braun. 2012. "L-Galactono-1,4-Lactone Dehydrogenase (GLDH) Forms Part of Three Subcomplexes of Mitochondrial Complex I in *Arabidopsis thaliana*." *Journal of Biological Chemistry* 287: 14412–14419.
- Schimmeyer, J., R. Bock, and E. H. Meyer. 2016. "L-Galactono-1,4-Lactone Dehydrogenase Is an Assembly Factor of the Membrane Arm of Mitochondrial Complex I in *Arabidopsis*." *Plant Molecular Biology* 90: 117–126.
- Sheftel, A. D., O. Stehling, A. J. Pierik, et al. 2009. "Human Ind1, an Iron-Sulfur Cluster Assembly Factor for Respiratory Complex I." *Molecular and Cellular Biology* 29: 6059–6073.
- Soufari, H., C. Parrot, L. Kuhn, F. Waltz, and Y. Hashem. 2020. "Specific Features and Assembly of the Plant Mitochondrial Complex I Revealed by Cryo-EM." *Nature Communications* 11: 5195. <https://www.nature.com/articles/s41467-020-18814-w>.
- Stroud, D. A., E. E. Surgenor, L. E. Formosa, et al. 2016. "Accessory Subunits Are Integral for Assembly and Function of Human Mitochondrial Complex I." *Nature* 538: 123–126.
- Subrahmanian, N., A. D. Castonguay, C. Remacle, and P. P. Hamel. 2020. "Assembly of Mitochondrial Complex I Requires the Low-Complexity Protein AMC1 in *Chlamydomonas reinhardtii*." *Genetics* 214: 895–911.
- Subrahmanian, N., C. Remacle, and P. P. Hamel. 2016. "Plant Mitochondrial Complex I Composition and Assembly: A Review." *Biochimica et Biophysica Acta* 1857: 1001–1014.
- Sunderhaus, S., N. V. Dudkina, L. Jansch, et al. 2006. "Carbonic Anhydrase Subunits Form a Matrix-Exposed Domain Attached to the Membrane Arm of Mitochondrial Complex I in Plants." *Journal of Biological Chemistry* 281: 6482–6488.
- Sung, A. Y., R. M. Guerra, L. H. Steenberge, et al. 2024. "Systematic Analysis of NDUFAF6 in Complex I Assembly and Mitochondrial Disease." *Nature Metabolism* 6: 1128–1142.
- van der Ven, A. T., A. Cabrera-Orefice, I. Wente, et al. 2023. "Expanding the Phenotypic and Biochemical Spectrum of NDUFAF3-Related Mitochondrial Disease." *Molecular Genetics and Metabolism* 140: 107675.
- Waltz, F., T.-T. Nguyen, M. Arrivé, et al. 2019. "Small Is Big in *Arabidopsis* Mitochondrial Ribosome." *Nature Plants* 5: 106–117.
- Waltz, F., R. D. Righetto, L. Lamm, et al. 2025. "In-Cell Architecture of the Mitochondrial Respiratory Chain." *Science* 387: 1296–1301.
- Wang, G., Y. Wang, J. Ni, et al. 2022. "An MCIA-Like Complex Is Required for Mitochondrial Complex I Assembly and Seed Development in Maize." *Molecular Plant* 15: 1470–1487.
- Wydro, M. M., P. Sharma, J. M. Foster, K. Bych, E. H. Meyer, and J. Balk. 2013. "The Evolutionarily Conserved Iron-Sulfur Protein INDH Is Required for Complex I Assembly and Mitochondrial Translation in *Arabidopsis* [Corrected]." *Plant Cell* 25: 4014–4027.
- Yin, Z., A.-N. A. Agip, H. R. Bridges, and J. Hirst. 2024. "Structural Insights Into Respiratory Complex I Deficiency and Assembly From the Mitochondrial Disease-Related ndufs4^{-/-} Mouse." *EMBO Journal* 43: 225–249.
- Zhou, L., M. Maldonado, A. Padavannil, F. Guo, and J. A. Letts. 2022. "Structures of Tetrahymena's Respiratory Chain Reveal the Diversity of Eukaryotic Core Metabolism." *Science* 376: 831–839.

Supporting Information

Additional supporting information can be found online in the Supporting Information section.

Figure S1. Synthetic *NDUFAF3* gene (Cre12.g496800) of *C. reinhardtii*.

A. Nucleotide sequence (<https://phytozome-next.jgi.doe.gov/> *Chlamydomonas reinhardtii* v5.6). Grey background: promoter region; yellow background: 5' and 3'UTR; blue background: coding sequence; green letters: first intron of RBCS2; underlined in bold and black: **ATG** (start codon), **TGA** (stop codon), and putative polyadenylation site (**TGTAA**); in bold and italics: *PstI* (**CTGCAG**) and *XbaI* (**TCTAGA**) restriction sites. The 3xFLAG addition is underlined in blue. **B.** Amino acid sequence of the NDUFAF3 protein. The 3xFLAG sequence is in bold.

A.

---NdeI---

```
TCTCGCGCTAGCCCACTGCGGTCGGTCCCCTGGTCTACTAAGTTTGTAAATGTGATTAAACACAACTGGAGTAGGACACCAAATTGACCCAAGCTGT
GTATGGCGGAGACAACACGATTTTGC GCGATGGCTCCATCCCGGCAAACCTCGCTCTTGTGTGCTCAAAGTTTCTTATACTGCGTGTGCAACGTAAT
ACATACACCATGCGTCAAAGCTCCCTCTTGCTGGCTGGGTCACTAGGTCGCGCGCTTGTTCGGGGCGCACGTTGCCGAGCTCAGCGCAGCTACGCTAA
GCAGCCGAGCGGCATCGCTGCATACATGTGAAGCGTCTTGTTCCTCCCGCTGCACGGGCGCGGGCGCGCAGCAGCGGGCCAGCGCTGACCGGACAAAC
ATGGGGTGGGGCCGCTGCAACACCCACGACAGCGCGAGCGCTGCACGCCGCCGGTCTCCAGCTCCAGTCGCGGCGGGGCGTACAGGGGTTTGACCGT
ATCGCAGAAACAGAGGCAGGCGAATTCATGGACTACAAGGACGACGATGACAAGGAATTCATGTCCAAAATGAGCGGCTATTACGCGGGCGGGT
TCTACATCAACAACGTACAGGTGAGTCGACGAGCAAGCCCGCGGATCAGGCAGCGTGCTTGACGATTTGACTTGCAACGCCCGCATTTGTGTCGACG
AAGGCTTTTGGCTCCTCTGTGCTGTCTCAAGCAGCATCTAACCTGCGTCGCGCTTTCCATTTGCAGGTGCCGGGCTCTGTGTTGGTGTGCGACGA
CATGTACTTCATGTGGCGCCCCCGCGCATCTCCGAGGTACGCCCGACAGCCTGATGCTGCTGGAGGTGCTCAAGCCCGCGCCTGAGGTGCTGGTG
TTGGGCACAGGCGCCACGCCGAGAAGCTGCCGCCGGCGGTGCGCGAGTACCTGCAGCGGCTGGGCATGCGCGTGGAGGTGCTGGACAGCCGCAACG
CCACCGGCTACTTCAACGTGCTCAATGACGAGGGCCGCGCGTGGTGGGCGCGCTGCTAGTGGCGGACCCGAGGCGCGCATGCCGAGAACCTGCC
AGACGCGCAGGAGCCGCTGTGGGACCGCGCCCCGCTCATGCAGCGCAGCGGCACCATCGACTACAAGGACCAGCAGCGGTGACTACAAGGATCAGCAG
ATCGACTACAAGGATGATGACGATAAGTGAAGGCGGGAGGAGGGAGGTGGAGGAGGGGCTGGAGGAGGGAGTGCATGAGGGGGTGCATGAGGGCA
CTGGTTGGGGTTGAGGGGCGGCTTCGGGCAGGCCAGAGTGGTTCGCTGGGAGCAGTGAAGGTGGGGGCGAAGGCAACGTGGAAATAGGAATGTGCAGC
TAGGGTGCAGAGGCCAGGGCGGGTCATGGGTGAGCACATGGAGCAATGGGCACTGGGCGGCGAGGTGCAACACCCAGAACACAGCAGGAAATA
CGGCCCTTCTGCTCTTCGGCAGCGGTGGCGGAAGTGGCGCAGGCGGCGACACCACCGATGTGCGCAAGTTGGAGCTGCGGGTCTGTTGATGAA
GCACGAGGCGATGGAGGGCGTGTGTCTGGGTGGATTGTAAAGGGGAAGGATTAGGGACAGCGGATGCAGAAAGGGCAGCTTCTCTAGTTTCTCCG
GTGCTGGTGGGTGACAGACTGGCTGGAGCACCTCTAGA
```

B.

NDUFAF3-3xFLAG

MSKMSGYYAGGFYINNVQVPGSVLVSHDMYFMWRPRRISEVTPDSLMLLEVLPKPAPEVLVLGTGATPQK
LPPAVREYLQRLGMRVEVLDSRNATGYFNVLNDEGRAVVGALLVADPEARMPENLPDAQEPLWDRAPL
MQRSGTIDYKDHDGDYKDHDIDYKDDDDK

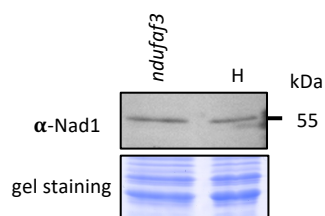


Figure S2. Nad1 is detected in the *ndufaf3* mutant strain.

Immunoblot of membrane fractions (20 μ g of proteins per lane) from the *ndufaf3* and H strains incubated with antibodies against Nad1. A Coomassie blue-stained gel loaded with the same extracts is shown as a control for loading. Note that this Coomassie blue staining is identical to the one presented in Fig. 1E, as the same membrane extracts are used.

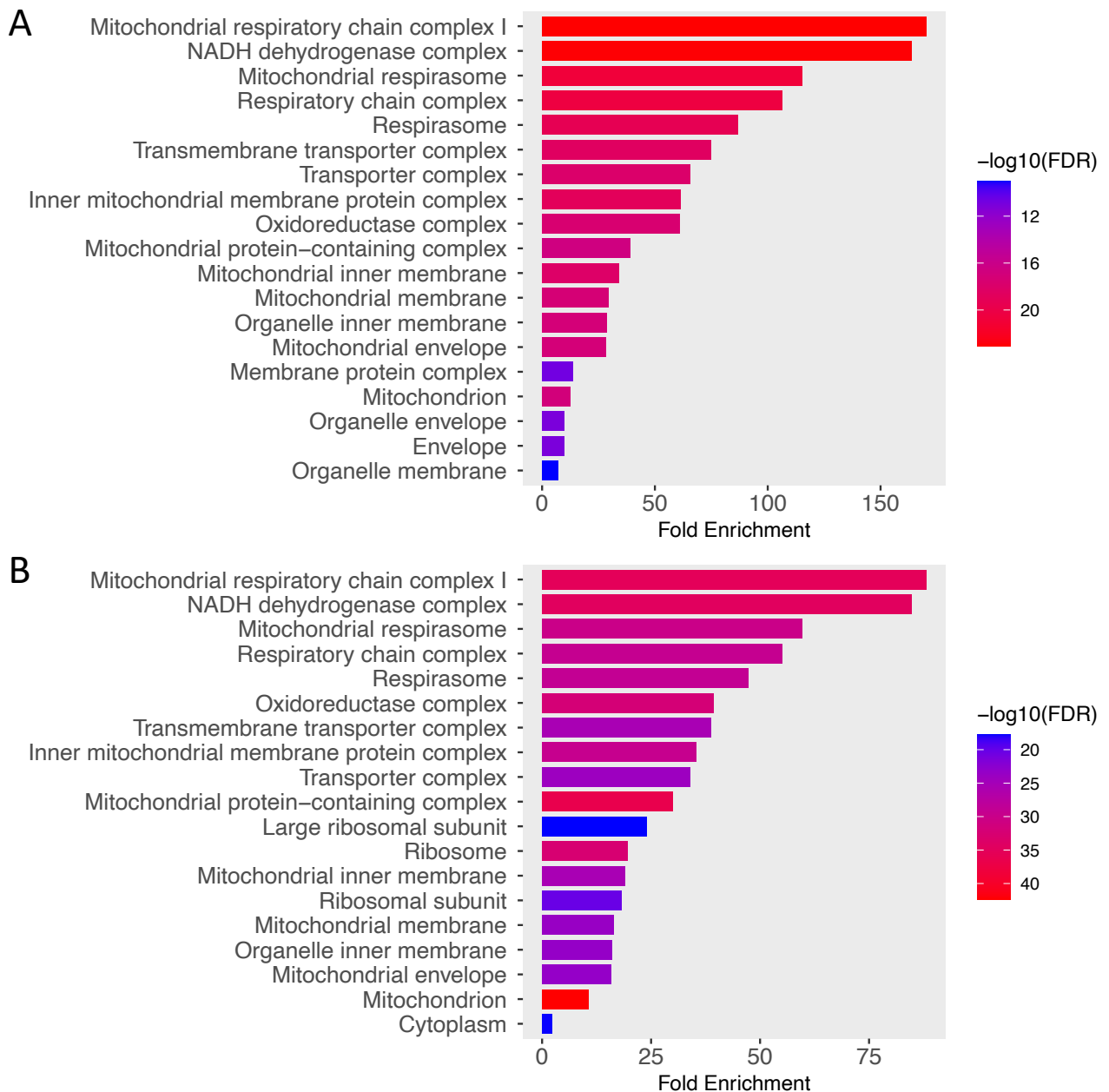


Figure S3. Functional analysis of proteins enriched by NDUFAF3 and TYKY co-immunoprecipitation

To perform the functional analysis of proteins enriched by NDUFAF3 (A) or TYKY (B) co-immunoprecipitation (coIP), we used ShinyGO v0.80 (<https://bioinformatics.sdstate.edu/go80/>) (1). Since ShinyGO relies on the *Chlamydomonas reinhardtii* genome annotation version 5.5, we first converted the protein IDs obtained from our IP experiments, which were based on version 6.1, to version 5.5. This conversion was carried out using the g:Profiler ID conversion tool (<https://biit.cs.ut.ee/gprofiler/convert>) (2). The conversion settings were as follows: Organism – *Chlamydomonas reinhardtii*; Target namespace – ENSG; Numeric IDs interpreted as ENTREZGENE.

For both NDUFAF3 and TYKY IP datasets, we selected proteins with a Log2 fold change (Log2FC) > 3. The resulting protein IDs were submitted to g:Profiler for conversion. In the case of the NDUFAF3 IP dataset, 50 out of 52 proteins were successfully converted to version 5.5 IDs. For the TYKY IP dataset, 164 out of 167 proteins were converted.

These converted IDs were subsequently analyzed in ShinyGO v0.80 using default parameters, with the “GO Cellular Component” ontology selected as the pathway database. Results were visualized based on Fold Enrichment and $-\log_{10}(\text{FDR})$ values.

Fold Enrichment quantifies the magnitude of enrichment, with higher values indicating a greater overrepresentation of a category and serving as an indicator of effect size.

P-values assess the statistical significance of the enrichment, with lower values indicating a lower probability that the observed result is due to random chance under the null hypothesis.

FDR q-values represent the False Discovery Rate-adjusted p-values, accounting for multiple hypothesis testing and reducing the likelihood of Type I errors.

References

- Ge, S.X., Jung, D. and Yao, R., 2020. ShinyGO: a graphical gene-set enrichment tool for animals and plants. *Bioinformatics*, 36(8), pp.2628-2629.
- Liis Kolberg, Uku Raudvere, Ivan Kuzmin, Priit Adler, Jaak Vilo, Hedi Peterson: g:Profiler-interoperable web service for functional enrichment analysis and gene identifier mapping (2023 update) *Nucleic Acids Research*, May 2023; doi:10.1093/nar/gkad347.

coIP TYKY

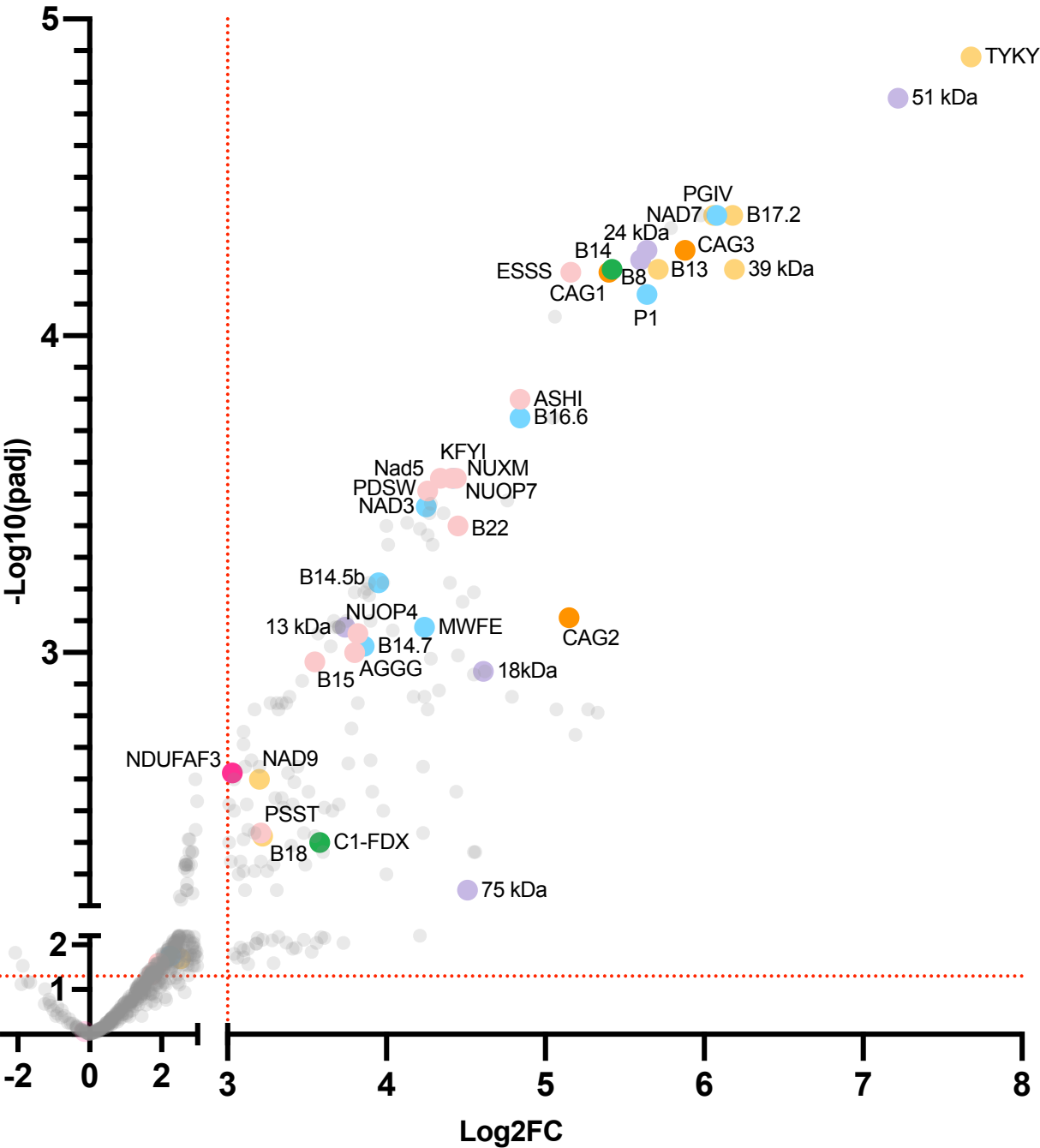


Figure S4. Volcano plot illustrating the global enrichment of proteins identified through co-immunoprecipitation performed with purified mitochondria from the NDUFAF3-3xFLAG-tagged strain, in the presence of TYKY antibodies or without antibodies as a control (n=3).

The x-axis displays the Log_2 fold change (Log_2FC), while the y-axis represents the $-\text{Log}_{10}$ of the adjusted p -value ($-\text{Log}_{10}(\text{padj})$), obtained using the IPInquiry4 R software package. Significantly enriched proteins are defined by a $\text{Log}_2\text{FC} > 3$ and a $-\text{Log}_{10}(\text{padj}) > 1.3$ (corresponding to an adjusted p -value ≤ 0.05), as indicated by the red axes. NDUFAF3 is marked as a red dot, with N module subunits shown in violet, Q module subunits in yellow, P_p module subunits in blue, P_d module subunits in pink, the subunits of the γ carbonic anhydrase domain in orange, and the ferredoxin bridge subunits in green (see **Table S2**). The complete datasets and analysis can be found in **Tables S1 and S3**.

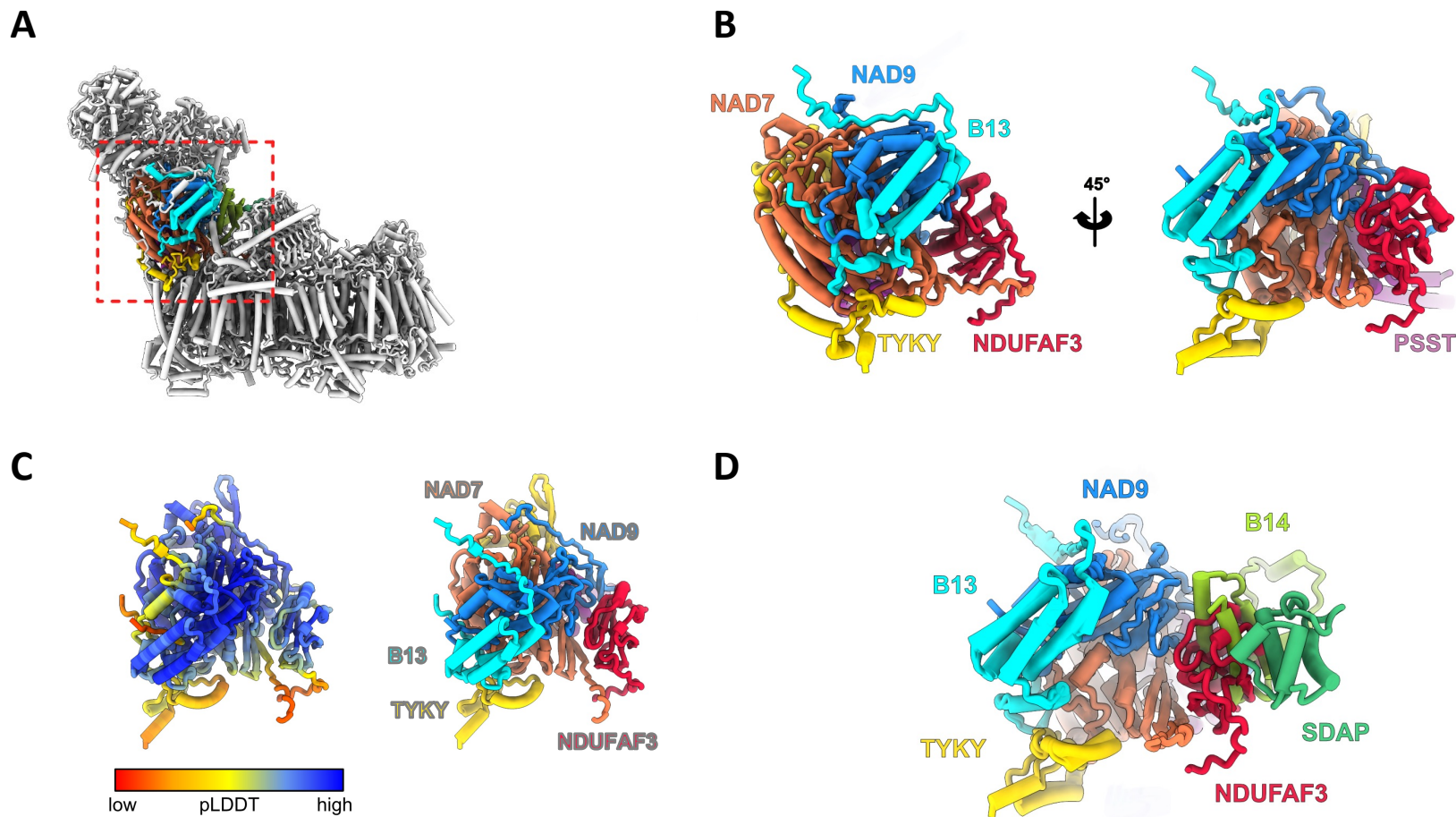


Figure S5. Structure prediction of the Q module of *Chlamydomonas* in complex with NDUFAF3.

A. Overall view of the mature complex I (*Chlamydomonas* model PDB: 9FRY). The subunits of the Q module are colored, and the dashed square indicates the zoomed-in view shown in **B**. **B.** The predicted model of the *Chlamydomonas* Q module subunits and NDUFAF3, generated by AlphaFold2 Multimer. **C.** pLDDT score for the AlphaFold2 Multimer prediction. Amino acid residues in the predicted model are colored according to their pLDDT score; the higher the score, the more confident the prediction is. Most of the model is predicted with high confidence, except for the C and N terminal parts of the proteins, which is expected. **D.** *Chlamydomonas* AlphaFold prediction overlaid with the *Chlamydomonas* model. NDUFAF3 clashes with subunits B14 and SDAP, which connect the matrix and membrane arms via the ferredoxin bridge.